6-2018

A Terbium Chlorobismuthate(III) Double Salt: Synthesis, Structure, and Photophysical Properties

John C. Ahern

Aaron D. Nicholas

Andrew W. Kelly

Benny Chan

Robert D. Pike

See next page for additional authors

Authors

John C. Ahern, Aaron D. Nicholas, Andrew W. Kelly, Benny Chan, Robert D. Pike, and Howard Patterson

A Terbium Chlorobismuthate(III) Double Salt: Synthesis, Structure, and Photophysical Properties

John C. Ahern,[a‡] Aaron D. Nicholas,[a] Andrew W. Kelly,[b] Benny Chan,[c] Robert D. Pike[b] and Howard H. Patterson*[a]

[a]*Chemistry Department, University of Maine. Orono, ME 04469 USA.;* [b]*Chemistry Department, College of William & Mary. Williamsburg, VA 23187 USA.;* [c]Chemistry Department, College of New Jersey. Ewing, NJ 08628-0718 USA.

*Corresponding Author: Howard H. Patterson
E-mail: howardp@maine.edu

Keywords: luminescence; crystallography; rare-earths; iodobismuthate; energy transfer

Abstract

We report on the structure and luminescence of a double salt trivalent rare earth ion acceptor, Tb^{3+}, with octahedral $[BiCl_6]^{3-}$ donor clusters. The novel $TbBiCl_6 \cdot 14H_2O$ (**1**) was prepared from aqueous BiOCl and $TbCl_3 \cdot 6H_2O$. The crystal structure of compound **1** exhibits isolated $[BiCl_6]^{3-}$ and $[Tb(OH_2)_8]^{3+}$ clusters. Luminescence data show energy transfer from octahedral chlorobismuthate(III) clusters to rare earth metal ions. Density Functional Theory (DFT) calculations show distinctly different emission pathways at high and low excitation energies.

1. Introduction

Rare earth metal ions produce sharp emission bands making them particularly useful in a variety of applications, including optoelectronics, biosensors, and photovoltaic compounds.[1–7] The challenge in developing viable materials using these ions centers on the difficulty of excitation of the lanthanide *f* electrons. The *f* orbitals are held close to the nucleus below the *d* orbitals due to lanthanide contraction and *f-f* transitions are symmetrically forbidden.[8] This results in weak emission intensities from these ions. Much research has focused on improving the emission intensity of solid state crystals [9–11] Energy transfer to rare earth metal centers is a possible avenue

of approach in achieving bright emission.[12,13] As an example, work by our group and Leznoff *et al.* have shown that rare earth ion emission can be tuned via changes in the bonding of coordinated d^{10} $Au(CN)_2^-$ ligands.[1,2,5,14,15] More specifically, we have discovered that the presence or absence of metallophilic Au-Au interactions has an effect on the emission intensity of the rare earth center. This change in emission occurs due to changes to the charge-transfer pathway whereby energy is transferred from the $Au(CN)_2^-$ anion to the rare earth ion.

Currently, our group is interested in rare earth excitation via post-transition halobismuthate(III) ions because of the large number of crystal motifs that halobismuthate(III) complexes are able to form. Complex halobismuthate(III) anions such as $[Bi_2Cl_{10}]^{2-}$, $[Bi_4Cl_{18}]^{6-}$, and $\{[Bi_2Cl_8]^{2-}\}_\infty$ with various organic cations have been reported.[16–26] These anions are composed of $[BiCl_6]^{3-}$ octahedra with various degrees of μ-Cl bridging. We have reported on simple alkali chlorobismuthate double salts.[13] These double salts form highly networked structures of chloride-bridged metal cations whose structures are dependent on the choice of alkali metal cation. Based on these findings we have been interested in the capacity of halobismuthate(III) complexes to form network structures with photophysically active metal ions whereby energy transfer occurs from the $[BiCl_6]^{3-}$ anion to the neighboring ion. We believe this behavior is possible due to the extensive metal-metal bridging that occurs within the crystal lattice. We recently investigated possible energy transfer in mixed iodobismuthate(III)/iodocuprate(I) crystals coordinated to organic ligands which also contain halide bridge metal centers.[16] Theoretical calculations indicated that these absorption bands were primarily the result of a halide/metal-to-metal charge transfer between the Bi(III) and Cu(I) centers. Based on these findings it seems possible to induce photoluminescence in photophysically active centers via energy transfer between halobismuthate(III) anions and lanthanide(III) cations.

Herein, we report the synthesis, structural analysis, and photophysical properties of the double salt $TbBiCl_6 \bullet 14H_2O$, along with DFT and TD-DFT calculations to help interpret our findings. Solid state absorption measurements were carried out and showed significant overlap of the broad $[BiCl_6]^{3-}$ anion band with that of the sharp Tb(III) absorption bands. This is in agreement with luminescence measurements which reveal enhanced Tb(III) emission at 77 K. Experimental findings with theoretical support indicate that rare earth emission is to the result of energy transfer from the Bi(III) metal center via the bridging chloride ions.

2. Experimental

2.1 Synthesis and Analysis of $TbBiCl_6$•$14H_2O$ (1). All reagents were purchased from Aldrich or Acros and used without purification. Terbium(III) hexachlorobismuthate(III) tetrakaidecahydrate (**1**) was synthesized by combining BiOCl (5 mL 0.25 M in conc. aq. HCl) and aq. $TbCl_3$•$6H_2O$ (5 mL 0.25 M). The filtered solution was slowly evaporated to yield pale yellow plates (**1**, 88.5%). Thermogravimetric analyses (TGA) (Figure S1 (SI)) were conducted using a TA Instruments Q500 in the dynamic (variable temp.) mode with a maximum heating rate of 50 ^oC/min. to 300 ^oC under 60 mL/min. N_2 flow. Compound **1** was analyzed for its Bi content via flame atomic absorption spectroscopy (AAS) using a PerkinElmer AAnalyst 700 instrument, confirming the formula derived from the X-ray crystallography. Samples were dissolved in 7% nitric acid (by weight) and then diluted in water to a concentration of 0.100 g/L. Blank solutions were made and their signal was subtracted from the sample scans. All scans were run three times with identical results. Experimental Bi content 26.2% (Theo. 25.1%).

2.2 X-ray Analysis. X-ray quality crystals were produced by partial evaporation of the aqueous solutions described above. The single crystal determination was carried out using a Bruker *SMART Apex II* diffractometer using graphite-monochromated Mo Kα radiation.[27] Data for the complexes were collected at 100 K. The data were corrected for Lorentz and polarization[28] effects and absorption using *SADABS*.[29] The structure was solved by use of direct methods. Least squares refinement on F^2 was used for all reflections. Structure solution, refinement and the calculation of derived results were performed using the *SHELXTL*[30] package of software. The non-hydrogen atoms were refined anisotropically. All hydrogen atoms were placed in theoretical positions.

2.3 Photophysical Measurements. Steady-state luminescence scans were run on **1** at 77 K. Compound **1** does not emit at temperatures above 90 K, so no room temperature scans were included. Spectra were taken with a Quantamaster-1046 photoluminescence spectrometer from Photon Technology International. This device uses a 75W xenon arc lamp combined with two excitation monochromators and one emission monochromator to adjust the bandwidth of light hitting the sample and detector, respectively. Signal intensity was measured using a photomultiplier tube. The samples were mounted on a copper plate using non-emitting copper-dust-high vacuum grease. Low-temperature scans were run on this system coupled to a Janis ST-

100 optical cryostat. Liquid nitrogen was used as coolant. Diffuse reflectance spectra (DRS) were collected on solid samples at 298 K. The light source was a Mikropack DH-2000 deuterium and halogen light source coupled with an Ocean Optics USB4000 detector. Scattered light was collected with a fiber optic cable. Spectra were referenced with PTFE. Data were processed using SpectraSuite 1.4.2_09.

2.4 Theoretical Calculations. DFT calculations were performed using the Gaussian '09 Software (Gaussian Inc.) hosted by the University of Maine Advanced Computing Group.[31] Ground state geometries and molecular orbital calculations were performed using the hybrid density functional theory due to Becke's 3-parameter nonlocal exchange functional with the nonlocal correlation functional of Lee, Yang and Parr, B3LYP and the basis set SDD for all atoms.[32–34] Molecular orbital calculations were performed on the ground state. The Avogadro software 1.2.0 was utilized for molecular orbital visualization.[35] To best model the electronic properties of **1** we have performed calculations on a single cluster composed of a $[BiCl_6]^{3-}$ octahedron and $[Tb(OH_2)_8]^{3+}$ square antiprism center as shown in Scheme 1 with the overall charge of the model being neutral. The X-ray structure coordinates were used as input for the initial geometry.

Scheme 1. A neutral model cluster of **1** composed of a $[BiCl_6]^{3-}$ octahedron and $[Tb(OH_2)_8]^{3+}$ square antiprism center.

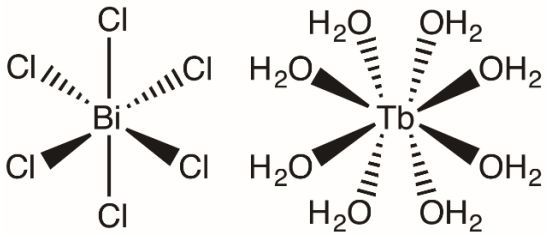

3. Results and Discussion

3.1 Structural Results. The crystal structure of **1** (Fig. 1) revealed isolated $[BiCl_6]^{3-}$ octahedra (Bi−Cl range = 2.571(5)-2.775(4) Å, *cis*-Cl−Bi−Cl range = 82.69(12)-98.9(2)°) and $Tb(OH_2)_8$ square antiprisms (Tb−O range = 2.318(13)-2.470(12) Å, *cis*-O−Tb−O angle range = 70.0(5)-81.3(3)°). These bismuth octahedra appear similar to those seen in previous reports of bismuth-chloride complexes.[17,36–38] Three of the Cl and four of the bound H_2O ligands show site disorder. In addition, six non-coordinated water molecules were present. A series of O−H···Cl and O−H···O hydrogen bonds produces a 3-D network (Fig 2). This bridging of the bismuth-chloride center to

the terbium-H_2O center may allow for energy transfer from the bismuth cluster to the terbium ion. Additional crystallographic details are given in Tables S1-6. Thermogravimetric analysis of **1** revealed dehydration producing $TbBiCl_6 \cdot 7H_2O$ and $TbBiCl_6$ phases (Fig. S1); $TbBiCl_6 \cdot 7H_2O$ was produced on vacuum drying of **1**. The expected Bi content for **1** was confirmed via AAS.

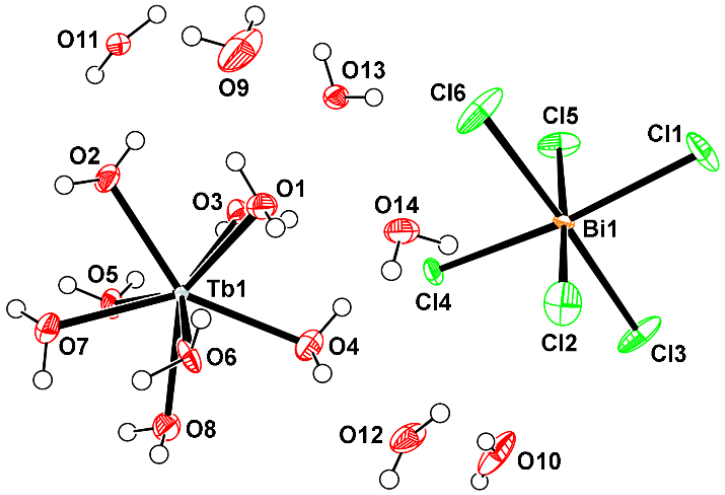

Fig. 1 Thermal ellipsoid (50%) drawing of the crystallographically independent unit in **1** (secondary locations of disordered O and Cl atoms omitted for clarity).

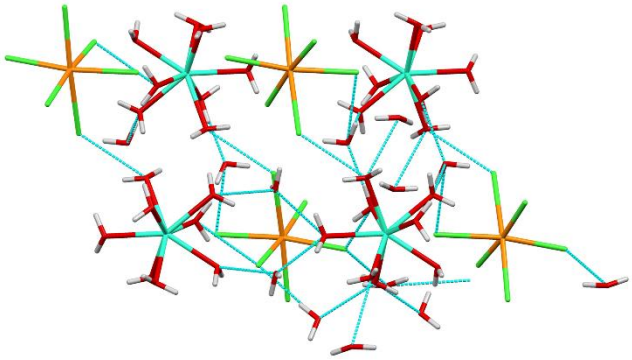

Fig. 2 Hydrogen bonding in **1** viewed along the *b*-axis (orange = Bi, green = Cl, turquoise = Tb, red = O, white = H).

3.2 Diffuse Reflectance Spectroscopy. Diffuse reflectance spectra of **1** were measured from crystals at room temperature (Fig. 3). A strong absorption band was observed at wavelengths less than ~380 nm with a weaker absorption noted between 380 nm and 530 nm. The sharp drop in absorption indicates an optical band edge at 388 nm. For comparison we measured the reflectance

of terbium(III) nitrate hexahydrate, which showed the characteristic rare earth emission bands at 542 nm and absorption bands from 325 nm to 390 nm. Interestingly, the reflectance of **1** does not display these *f-f* absorption peaks and instead reveals only a single broad absorption band. We have assigned this broad band to the $[BiCl_6]^{3-}$ octahedral center as a Cl 3*p*→Bi 6*s* transition. This assignment is in agreement with other studies of $[BiCl_6]^{3-}$ complexes which describe these bands as chloride to bismuth(III) ligand-to-metal charge transfer (LMCT) and bismuth(III) metal-centered transition (MC).[39–41] The absorption band of the chlorobismuthate ion easily overlaps those of the terbium(III) nitrate, indicating possible energy transfer from the $[BiCl_6]^{3-}$ anion to the rare earth $[Tb(OH_2)_8]^{3+}$ cluster.

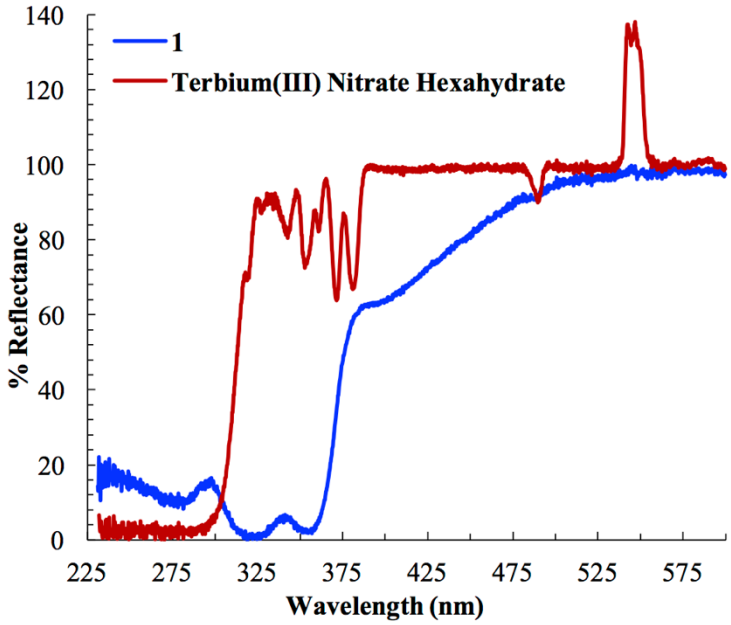

Fig. 3 Diffuse reflectance UV-vis spectra of **1** and terbium(III) nitrate hexahydrate.

3.3 Photophysical Results. Double salt **1** was examined via steady state luminescence spectroscopy at 77 K. The compound did not emit at temperatures above 90 K. Fig. 4 shows the steady state luminescence spectra for **1**. The annotations with arrows indicate the excitation/emission energy corresponding to the emission/excitation peaks, respectively. For Tb/Bi double salt **1** four emission peaks are observed. Each of these corresponds with a known emission of the Tb^{3+} ion.[1,2] However, a distinction exists between direct excitation of Tb^{3+} and the energy transfer from Bi^{3+} to Tb^{3+}. Under 351 nm excitation, Bi^{3+} may become excited and transfer energy to Tb^{3+}. The Tb^{3+} ion can also be excited directly at energies of 305, 358, 369 or 378 nm. The peak

centered at 584 nm is also partially the result of relaxation of the Bi^{3+} excited lattice via phonon-phonon interactions, in agreement with similar studies.[42,43] The observed emission band is broad since bismuth has a high-energy excited state and low-energy excited states corresponding with the high and low energy emissions, respectively. The energy transfer pathway is favored at 352 nm because *f* orbitals are difficult to excite directly, in contrast to *d* orbitals.[1,2,5,14] Octahedral bismuth-chloride centers undergo excitation of the chloride 2*p* to the bismuth 6*p*/chloride 3*s*, which constitutes a HOMO-LUMO transition.[36] This mechanism was first reported by Pelle *et al.* in $Cs_2NaBiCl_6$ crystal clusters.[36–38] Addition of the terbium ions offers an alternative emission pathway. Due to the forbidden nature of *f-f* transitions, we expect the excitation of **1** at these wavelengths to occur via bismuth. Such transitions are also reported by Pelle *et al.* who assigned the transition in the bismuth-chloride centers from the HOMO to the cation LUMO.[36–38] The bridging of the chlorobismuthate octahedron to the $[Tb(OH_2)_8]^{3+}$ center in **1** provides an important interface which may facilitate energy transfer by shifting the emission of the Bi^{3+} slightly so as to increase the spectral overlap between bismuth and terbium. This increased overlap allows for greater Förster energy transfer.[44] Table 1 shows state assignments for **1**.

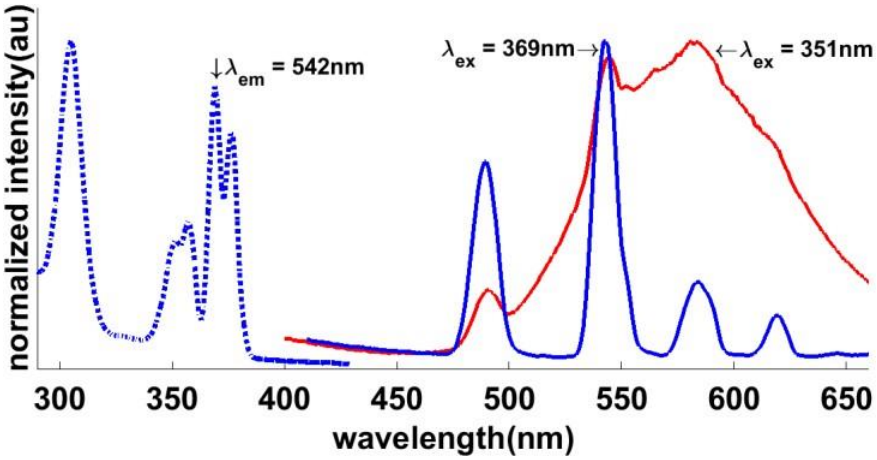

Fig. 4 Steady state luminescence spectra for **1** at 77 K. The annotations indicate the excitation/emission energy that corresponds with the selected emission/excitation peaks, respectively.

Table 1 Observed emission maxima for **1** at 77 K. Note: Tb^{3+} can also be directly excited at 305, 358, 369 and 378nm.

λ_{em} (nm), [λ_{ex} (nm)]	Stokes Shifts (cm^{-1})	Assignment
490, [351]	8,080	$^5D_4 \rightarrow {}^7F_6$ energy transfer
542, [351]	10,000	$^5D_4 \rightarrow {}^7F_5$ energy transfer
584, [351]	11,400	$^5D_4 \rightarrow {}^7F_4$ energy transfer
619, [351]	12,300	$^5D_4 \rightarrow {}^7F_3$ energy transfer

3.4 DFT Calculations. DFT calculations have been performed on a single $[Tb(OH_2)_8][BiCl_6]$ unit (Fig. 5) to explore the electronic transitions responsible for the observed luminescence behavior at different excitation energies. Ground state calculations produce a structure that is in general agreement with experimental X-ray studies (Bi−Cl range = 2.562-2.818 Å, *cis*-Cl−Bi−Cl range = 89.2-93.7°, Tb−O range = 2.398-2.541 Å, *cis*-O−Tb−O angle range = 63.8-79.9°). In this ground state both the octahedral $[BiCl_6]^{3-}$ and square antiprismatic $[Tb(OH_2)_8]^{3+}$ geometries are preserved. Also preserved in this ground state calculation are the close Cl···H distances (2.047-2.482 Å) which are important in our consideration of energy transfer from the chlorobismuthate anion to the terbium ion center.

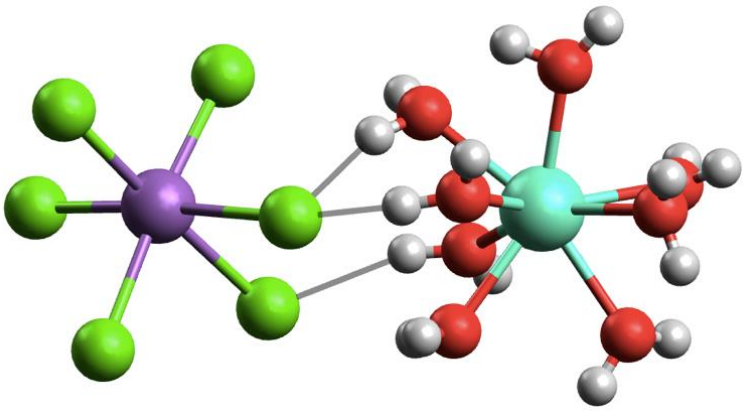

Fig. 5 B3LYP/SDD calculated ground state of $[Tb(OH_2)_8][BiCl_6]$. Close Cl···H interactions shown in gray.

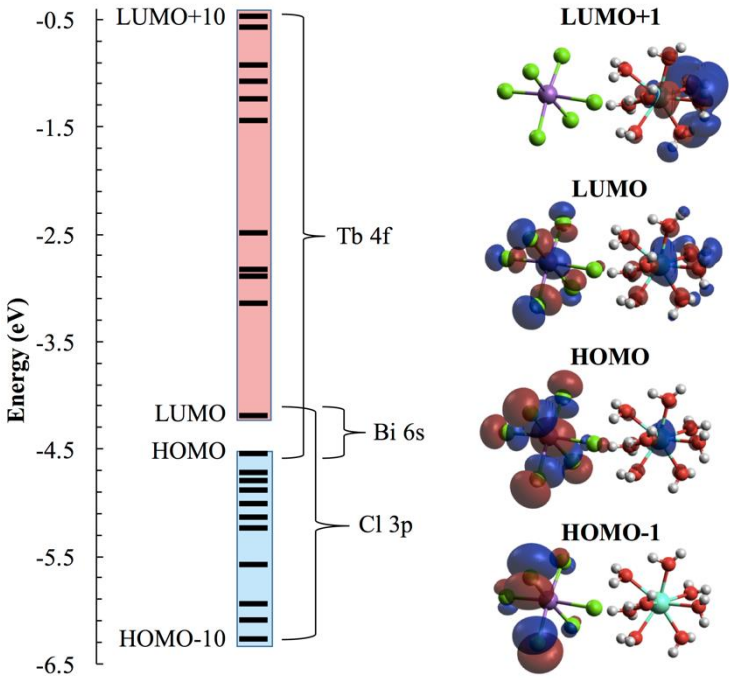

Fig. 6 Molecular orbitals diagram (**left**) and isodensity representations (**right**) of the frontier molecular orbitals in **1**.

Isodensity representations of the frontier molecular orbitals in **1** are presented in Fig. 6. The higher-lying occupied molecular orbitals are primarily composed of the Cl 3*p* atomic orbitals, with significant contribution of the Bi 6*s* to the HOMO. A small contribution from the Tb 4*f* atomic orbital to the HOMO is also observed. The LUMO has significant contributions from the Bi 6*s*, Cl 3*p*, and Tb 4*f*. The remaining low-lying unoccupied molecular orbitals are composed of the Tb 4*f* atomic orbitals. In the luminescence spectra at low energies only rare earth *f*-*f* peaks are observed. In this case electrons most likely are promoted from the HOMO to unoccupied MOs other than the LUMO. In the case of high energy excitation, we observed both rare earth bands and a broad chlorobismuthate band which can only result from a Cl 3*p* → Bi 6*s* transition. According to the MO calculations, only the LUMO contains atomic orbitals for each of these transitions. Thus, at high energy excitation we expect that low-lying occupied MO electrons to be excited to the LUMO band. Since these low-lying MOs are composed only on the Cl 3*p*, this transition constitutes a Cl 3*p* → Tb^{3+} energy transfer via a chlorobismuthate(III)/rare earth cluster-cluster interaction. With this in mind, we have developed an energy transfer mechanism which we believe describes the energy transfer processes at high and low energy excitation, shown in Fig. 7.

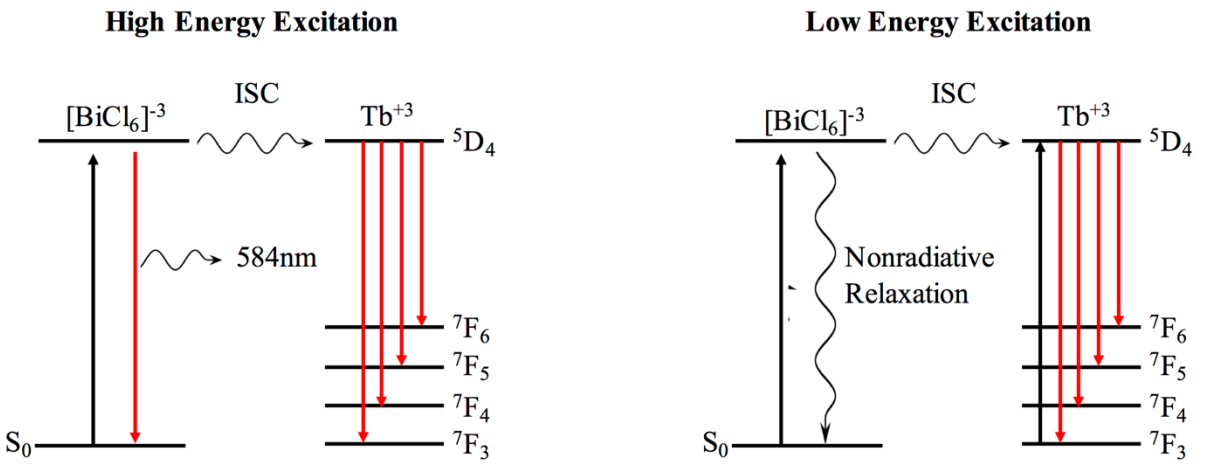

Fig. 7 Energy diagram of **1** at high and low energy excitation. At high energy excitation (<350 nm) energy absorbed by the chlorobismuthate cluster is reemitted at 584 nm and transferred to the rare earth cluster competitively. At low energy excitation (>370 nm) energy absorbed by the chlorobismuthate cluster is transferred to the rare earth cluster and undergoes non-radiative relaxation. (ISC = Intersystem system crossing).

4.1 Conclusions

The novel bismuth(III)/terbium(III) double salt $TbBiCl_6 \bullet 14H_2O$ (**1**) was synthesized and its crystal structure was determined. Compound **1** contains isolated $[BiCl_6]^{3-}$ and $[Tb(OH_2)_8]^{3+}$ units built within a network structure. Structural measurements reveal close Cl···H interactions between the bismuth and terbium ions, indicating the potential for energy transfer between centers. The broad absorption band observed in diffuse reflectance spectra are assigned to a Cl 3*p*→Bi 6*s* transition within the chlorobismuthate cluster. These transitions have been previously proposed by Pelle *et al.*[36–38] This $[BiCl_6]^{3-}$ absorption band strongly overlaps the sharp absorption bands of terbium(III). Luminescence experiments show enhanced rare earth ion emission from energy transfer between the excited $[BiCl_6]^{3-}$ anion and the $[Tb(OH_2)_8]^{3+}$ cation. We have supported our findings with DFT calculations.

Acknowledgements:

RDP thanks the National Science Foundation and the College of William and Mary for the purchase of X-ray equipment. JCA and HHP thank the USGS/WRRI for partial funding of this

research. The HHP group thanks the University of Maine Advanced Computing Group for their support and generous allocation of computing resources.

Notes and references

[a] *Chemistry Department, University of Maine. Orono, ME 04469 USA. Tel: 01 207 581 1178; Email: howardp@maine.edu*

[b] *Chemistry Department, College of William & Mary. Williamsburg, VA 23187 USA. Tel: 01 757 221 2555; Email: rdpike@wm.edu*

[c] *Chemistry Department, College of New Jersey. Ewing, NJ 08628-0718 USA. Tel: 01 609 771 2471; Email: chan@tcnj.edu*

† Electronic Supplementary Information (ESI) available: [details of any supplementary information available should be included here]. See DOI: 10.1039/b000000x/

‡Current Address: *Materials Recovery & Recycle Group (AMPP-4), Actinide Materials Processing & Power Division, Los Alamos National Laboratory, Los Alamos, NM 87545.* Los Alamos National Laboratory strongly supports academic freedom and a researcher's right to publish; as an institution, however, the Laboratory does not endorse the viewpoint of a publication or guarantee its technical correctness.

References

(1) Ahern, J. C.; Roberts, R. J.; Follansbee, P.; Lezno, D. B.; Patterson, H. H. Structure and Emissive Properties of Heterobimetallic Ln−Au Coordination Polymers: Role of Tb and Eu in Non-Aurophilic $[nBu_4N]_2[Ln(NO_3)_4Au(CN)_2]$ versus Aurophilic $Ln[Au(CN)_2]_3 \cdot 3H_2O/3D_2O$ Chains. *Inorg. Chem.* **2014**, *53* (3), 7571−7579.

(2) Roberts, R. J.; Li, X.; Lacey, T. F.; Pan, Z.; Patterson, H. H.; Leznoff, D. B. Heterobimetallic Lanthanide–gold Coordination Polymers: Structure and Emissive Properties of Isomorphous $[nBu_4N]_2[Ln(NO_3)_4Au(CN)_2]$ 1-D Chains. *Dalton Trans.* **2012**, *41* (23), 6992-6997 DOI: 10.1039/c2dt30156c.

(3) Liu, J.; Huang, L.; Tian, X.; Chen, X.; Shao, Y.; Xie, F.; Chen, D.; Li, L. Magnetic and Fluorescent Gd_2O_3:Yb^{3+}/Ln^{3+} Nanoparticles for Simultaneous Upconversion luminescence/MR Dual Modal Imaging and NIR-Induced Photodynamic Therapy. *Int. J. Nanomedicine* **2016**, *12*, 1–14 DOI: 10.2147/IJN.S118938.

(4) Wang, Y.; Yang, Z.; Ma, Y.; Chai, Z.; Qiu, J.; Song, Z. Upconversion Emission

Enhancement Mechanisms of Nd^{3+} -Sensitized $NaYF_4$:Yb^{3+},Er^{3+} Nanoparticles Using Tunable Plasmonic Au Films: Plasmonic-Induced Excitation, Radiative Decay Rate and Energy-Transfer Enhancement. *J. Mater. Chem. C* **2017**, *5*, 8535-8544 DOI: 10.1039/C7TC02374J.

(5) Garcia, Y.; Su, B. L.; Roberts, R. J.; Ahern, J. C.; Patterson, H. H.; Leznoff, D. B. Ce/$Au(CN)_2^-$-Based Coordination Polymers Containing and Lacking Aurophilic Interactions. *Eur. J. Inorg. Chem.* **2016**, *2016* (13–14), 2082–2087 DOI: 10.1002/ejic.201600174.

(6) Cunha-Silva, L.; Lima, S.; Ananias, D.; Silva, P.; Mafra, L.; Carlos, L. D.; Pillinger, M.; Valente, A. A.; Almeida Paz, F. A.; Rocha, J. Multi-Functional Rare-Earth Hybrid Layered Networks: Photoluminescence and Catalysis Studies. *J. Mater. Chem.* **2009**, *19* (17), 2618-2632 DOI: 10.1039/b817381h.

(7) Auzel, F.; Pecile, D.; Morin, D. Rare Earth Doped Vitroceramics: New, Efficient, Blue and Green Emitting Materials for Infrared Up-Conversion. *J. Electrochem. Soc.* **1975**, *122* (1), 101-107 DOI: 10.1149/1.2134132.

(8) Loh, E. Lowest 4f→5d Transition of Trivalent Rare-Earth Ions in CaF_2 Crystals. *Phys. Rev.* **1966**, *147* (1), 332–335 DOI: 10.1103/PhysRev.147.332.

(9) Binnemans, K. Lanthanide-Based Luminescent Hybrid Materials. *Chem. Rev.* **2009**, *109* (9), 4283–4374 DOI: 10.1021/cr8003983.

(10) Zhou, J.; Liu, Q.; Feng, W.; Sun, Y.; Li, F. Upconversion Luminescent Materials: Advances and Applications. *Chem. Rev.* **2015**, *115* (1), 395–465 DOI: 10.1021/cr400478f.

(11) Eliseeva, S. V.; Bünzli, J.-C. G. Lanthanide Luminescence for Functional Materials and Bio-Sciences. *Chem. Soc. Rev.* **2010**, *39* (1), 189–227 DOI: 10.1039/B905604C.

(12) Shavaleev, N. M.; Moorcraft, L. P.; Pope, S. J. A.; Bell, Z. R.; Faulkner, S.; Ward, M. D. Sensitized Near-Infrared Emission from Complexes of Yb(III), Nd(III), and Er(III) by Energy-Transfer from Covalently Attached Pt II -Based Antenna Units. *Chem. Eur. J.* **2003**, *9*, 5283–5291 DOI: 10.1002/chem.200305132.

(13) Baca, S. G.; Pope, S. J. A.; Adams, H.; Ward, M. D. Cyanide-Bridged Os(II)/Ln(III) Coordination Networks Containing $[Os(phen)(CN)_4]^{2-}$ as an Energy Donor: Structural and Photophysical Properties. *Inorg. Chem.* **2008**, *47* (9), 3736–3747 DOI: 10.1021/ic702353c.

(14) Roberts, R. J.; Le, D.; Leznoff, D. B. Color-Tunable and White-Light Luminescence in Lanthanide–Dicyanoaurate Coordination Polymers. *Inorg. Chem.* **2017**, *56* (14), 7948–7959 DOI: 10.1021/acs.inorgchem.7b00735.

(15) Arthur, R. B.; Nicholas, A. D.; Roberts, R. J.; Assefa, Z.; Leznoff, D. B.; Patterson, H. H. Luminescence Investigation of Samarium(III)/Dicyanoaurate(I)-Based Coordination Networks with and without Aurophilic Interactions. *Gold Bull.* **2017**, 1-10 DOI: 10.1007/s13404-017-0221-0.

(16) Kelly, A. W.; Wheaton, A. M.; Nicholas, A. D.; Barnes, F. H.; Patterson, H. H.; Pike, R. D. Iodobismuthate(III) and Iodobismuthate(III)/Iodocuprate(I) Complexes with Organic Ligands. *Eur. J. Inorg. Chem.* **2017**, *43*, 4990-5000 DOI: 10.1002/ejic.201701052.

(17) Kelly, A. W.; Nicholas, A.; Ahern, J. C.; Chan, B.; Patterson, H. H.; Pike, R. D. Alkali Metal Bismuth(III) Chloride Double Salts. *J. Alloys Compd.* **2016**, *670*, 337–345 DOI: 10.1016/j.jallcom.2016.02.055.

(18) Adonin, S. A.; Rakhmanova, M. I.; Samsonenko, D. G.; Sokolov, M. N.; Fedin, V. P. Hybrid Salts of Binuclear Bi(III) Halide Complexes with 1,2-Bis(pyridinium)ethane Cation: Synthesis, Structure and Luminescent Behavior. *Inorganica Chim. Acta* **2016**, *450*, 232–235 DOI: 10.1016/j.ica.2016.06.010.

(19) Blažič, B.; Lazarini, F. Structure of Diethylammonium Tetrachlorobismuthate(III). *Acta Crystallogr. Sect. C Cryst. Struct. Commun.* **1985**, *41* (11), 1619–1621 DOI: 10.1107/S0108270185008782.

(20) Huang, G.; Sun, Y.-Q.; Xu, Z.; Zeller, M.; Hunter, A. D. Structural Regularity and Diversity in Hybrids of Aromatic Thioethers and $BiBr_3$: From Discrete Complexes to Layers and 3D Nets. *Dalton Trans.* **2009**, No. 26, 5083-5093 DOI: 10.1039/b902490p.

(21) Xu, G.; Guo, G.-C.; Wang, M.-S.; Zhang, Z.-J.; Chen, W.-T.; Huang, J.-S. Photochromism of a Methyl Viologen Bismuth(III) Chloride: Structural Variation Before and After UV Irradiation. *Angew. Chemie Int. Ed.* **2007**, *46* (18), 3249–3251 DOI: 10.1002/anie.200700122.

(22) Bowmaker, G. A.; Harrowfield, J. M.; Junk, P. C.; Skelton, B. W.; White, A. H. Syntheses, Structures and Vibrational Spectra of Some Dimethyl Sulfoxide Solvates of Bismuth(III) Bromide and Iodide. *Aust. J. Chem.* **1998**, *51* (4), 285-292 DOI: 10.1071/C97035.

(23) Leblanc, N.; Bi, W.; Mercier, N.; Auban-Senzier, P.; Pasquier, C. Photochromism, Electrical Properties, and Structural Investigations of a Series of Hydrated Methylviologen Halobismuthate Hybrids: Influence of the Anionic Oligomer Size and Iodide Doping on the Photoinduced Properties and on the Dehydration Process. *Inorg. Chem.* **2010**, *49* (13), 5824–5833 DOI: 10.1021/ic901525p.

(24) Lin, R.-G.; Xu, G.; Wang, M.-S.; Lu, G.; Li, P.-X.; Guo, G.-C. Improved Photochromic Properties on Viologen-Based Inorganic–Organic Hybrids by Using π-Conjugated Substituents as Electron Donors and Stabilizers. *Inorg. Chem.* **2013**, *52* (3), 1199–1205 DOI: 10.1021/ic301181b.

(25) Lin, R.-G.; Xu, G.; Lu, G.; Wang, M.-S.; Li, P.-X.; Guo, G.-C. Photochromic Hybrid Containing In Situ -Generated Benzyl Viologen and Novel Trinuclear $[Bi_3Cl_{14}]^{5-}$: Improved Photoresponsive Behavior by the π···π Interactions and Size Effect of Inorganic Oligomer. *Inorg. Chem.* **2014**, *53* (11), 5538–5545 DOI: 10.1021/ic5002144.

(26) Belkyal, I.; Mokhlisse, R.; Tanouti, B.; Chanh, N. B.; Couzi, M. Phase Transitions in $(CH_3NH_3)_3Bi_2Cl_9$ Studied by Calorimetric, X-Ray Diffraction and Dielectric Methods. *J. Alloys Compd.* **1992**, *188*, 186–189 DOI: 10.1016/0925-8388(92)90672-V.

(27) *SMART Apex II, Data Collection Software*, version 2.1; Bruker AXS Inc.: Madison, WI, 2005.

(28) *SAINT Plus, Data Reduction Software*, version 7.34a; Bruker AXS Inc.: Madison, WI, 2005.

(29) Sheldrick, G.M. SADABS; University of Göttingen: Göttingen, Germany, 2005.

(30) Sheldrick, G.M. Acta Crystallogr. Sect. A 2008, 64, 112.

(31) Frisch, M. J. Trucks, G. W. Schlegel, H. B. Scuseria, G. E. Robb, M. A. Cheeseman, J. R. Scalmani, G. Barone, V. Mennucci, B. Petersson, G. A. Nakatsuji, H. Caricato, M. Li, X. Hratchian, H. P.. Izmaylov, A. F Bloino, J. Zheng, G. Sonnenberg, J. L. Hada, M. Ehara, M. Toyota, K. Fukuda, R. Hasegawa, J. Ishida, M. Nakajima, T. Honda, Y. Kitao, O. Nakai, H. Vreven, T. Montgomery, Jr., J. A. Peralta, J. E. Ogliaro, F. Bearpark, M. Heyd, J. J. Brothers, E. Kudin, K. N. Staroverov, V. N. Keith, T. Kobayashi, R. Normand, J. Raghavachari, K. Rendell, A. Burant, J. C. Iyengar, S. S. Tomasi, J. Cossi, M. Rega, N. Millam, J. M. Klene, M. Knox, J. E. Cross, J. B. Bakken, V. Adamo, C. Jaramillo, J. Gomperts, R. Stratmann, R. E. Yazyev, O. Austin, A. J. Cammi, R. Pomelli, C. Ochterski,

J. W. Martin, R. L. Morokuma, K. Zakrzewski, V. G. Voth, G. A. Salvador, P. Dannenberg, J. J. Dapprich, S. Daniels, A. D. Farkas, O. Foresman, J. B. Ortiz, J. V. Cioslowski, J. and Fox, D. J. Gaussian, Inc., Wallingford CT, 2010.

(32) Becke, A. D. Density-functional Thermochemistry. III. The Role of Exact Exchange. *J. Chem. Phys.* **1993**, *98* (7), 5648–5652 DOI: 10.1063/1.464913.

(33) Lee, C.; Yang, W.; Parr, R. G. Development of the Colle-Salvetti Correlation-Energy Formula into a Functional of the Electron Density. *Phys. Rev. B* **1988**, *37* (2), 785–789 DOI: 10.1103/PhysRevB.37.785.

(34) Fuentealba, P.; Preuss, H.; Stoll, H.; Von Szentpály, L. A Proper Account of Core-Polarization with Pseudopotentials: Single Valence-Electron Alkali Compounds. *Chem. Phys. Lett.* **1982**, *89* (5), 418–422 DOI: 10.1016/0009-2614(82)80012-2.

(35) Hanwell, M. D.; Curtis, D. E.; Lonie, D. C.; Vandermeersch, T.; Zurek, E.; Hutchison, G. R. Avogadro: An Advanced Semantic Chemical Editor, Visualization, and Analysis Platform. *J. Cheminform.* **2012**, *4* (1), 17 DOI: 10.1186/1758-2946-4-17.

(36) Pelle, F.; Jacquier, B.; Denis, J. P.; Blanzat, B. Optical Properties of $Cs_2NaBiCl_6$. *J. Lumin.* **1978**, *17* (1), 61–72 DOI: 10.1016/0022-2313(78)90026-1.

(37) Pelle, F.; Denis, J.; Blanzat, B. Optical Properties of $Cs_2NaBiCl_6$. *J. Lumin.* **1981**, *24–25*, 127–130 DOI: 10.1016/0022-2313(81)90237-4.

(38) Pelle, F.; Blanzat, B.; Chevalier, B. Low Temperature Phase Transition in Cubic Elpasolithe Crystal $Cs_2NaBiCl_6$. *Solid State Commun.* **1984**, *49* (11), 1089–1093 DOI: 10.1016/0038-1098(84)90430-7.

(39) Ferjani, H.; Boughzala, H. New Quasi-One-Dimensional Organic-Inorganic Hybrid Material: 1,3-Bis(4-Piperidinium)propane Pentachlorobismuthate(III) Synthesis, Crystal Structure, and Spectroscopic Studies. *J. Mater.* **2014**, *2014*, 1–8 DOI: 10.1155/2014/253602.

(40) Walton, R. A.; Matthews, R. W.; Jørgensen, C. K. Absorption Spectra of Post-Transition Group Halide Complexes. *Inorganica Chim. Acta* **1967**, *1*, 355–359 DOI: 10.1016/S0020-1693(00)93201-8.

(41) Reisfeld, R.; Honigbaum, A. Diffusion of Bismuth Ions in Potassium Chloride Crystals. *J. Chem. Phys.* **1968**, *48* (12), 5565–5569 DOI: 10.1063/1.1668258.

(42) Tan, C.; Zhu, G.; Hojamberdiev, M.; Okada, K.; Liang, J.; Luo, X.; Liu, P.; Liu, Y. Co_3O_4

Nanoparticles-Loaded BiOCl Nanoplates with the Dominant {001} Facets: Efficient Photodegradation of Organic Dyes Under Visible Light. *Appl. Catal. B Environ.* **2014**, *152–153*, 425–436 DOI: 10.1016/j.apcatb.2014.01.044.

(43) Deng, Z.; Tang, F.; Muscat, A. J. Strong Blue Photoluminescence from Single-Crystalline Bismuth Oxychloride Nanoplates. *Nanotechnology* **2008**, *19* (29), 295705 DOI: 10.1088/0957-4484/19/29/295705.

(44) Baril-Robert, F.; Guo, Z.; Patterson, H. H. Study of the Energy Transfer Process in the Highly Luminescent Heterometallic Dimers of Ce^{3+} and d^{10} $[Ag(CN)_2]^-$ or d^8 $[Pt(CN)_4]^{2-}$ Ions. *Chem. Phys. Lett.* **2009**, *471* (4–6), 258–263 DOI: 10.1016/j.cplett.2009.02.039.